Stability versus maneuverability in hovering flight

Yangyang Huang, Monika Nitsche, and Eva Kanso

Citation: Physics of Fluids **27**, 061706 (2015); doi: 10.1063/1.4923314
View online: http://dx.doi.org/10.1063/1.4923314
View Table of Contents: http://scitation.aip.org/content/aip/journal/pof2/27/6?ver=pdfcov
Published by the AIP Publishing

PHYSICS OF FLUIDS **27**, 061706 (2015)

Stability versus maneuverability in hovering flight

Yangyang Huang,[1] Monika Nitsche,[2] and Eva Kanso[1,a)]
[1]*Aerospace and Mechanical Engineering, University of Southern California, Los Angeles, California 90089, USA*
[2]*Department of Mathematics and Statistics, University of New Mexico, Albuquerque, New Mexico 87131, USA*

(Received 29 March 2015; accepted 5 June 2015; published online 30 June 2015)

Insects and birds are often faced by opposing requirements for agile and stable flight. Here, we explore the interplay between aerodynamic effort, maneuverability, and stability in a model system that consists of a Λ-shaped flyer hovering in a vertically oscillating airflow. We determine effective conditions that lead to periodic hovering in terms of two parameters: the flyer's shape (opening angle) and the effort (flow acceleration) needed to keep the flyer aloft. We find optimal shapes that minimize effort. We then examine hovering stability and observe a transition from unstable, yet maneuverable, to stable hovering. Interestingly, this transition occurs at post-optimal shapes, that is, at increased aerodynamic effort. These results have profound implications on the interplay between stability and maneuverability in live organisms as well as on the design of man-made air vehicles. © *2015 AIP Publishing LLC.* [http://dx.doi.org/10.1063/1.4923314]

The unsteady flow-structure interactions in flapping wing motions produce lift and thrust forces that allow insects and birds to fly forward or hover in place. The mechanisms responsible for the generation of these aerodynamic forces received a great deal of attention in recent experimental[1–6] and theoretical[7–13] studies, mostly emphasizing the importance of leading-edge and wake vorticity in force production.[14,15] However, the stability of flapping flight in response to environmental disturbances is less well explored.[16] Recent studies report conflicting accounts of intrinsic instability[17,18] and passive stability.[19,20]

Live organisms certainly employ active feedback control during flight,[21–24] but it is not clear to what extent. Active stabilization requires additional *effort* and thus energy expenditure. One can argue that passive stability reduces the effort required for flying. In this sense, it seems reasonable to conjecture that, from an evolutionary perspective, passive stability may have a positive selection value. However, stability can be thought of as "resistance to change" which conflicts with maneuverability.[21,23] Unlike stability, there is no clear quantitative definition of maneuverability, which we consider here to simply mean lack of stability. Lack of stability is a necessary but not sufficient condition for maneuverability. Stable motions require extra effort to change, which could make sudden maneuvers energetically costly, whereas an unstable motion only needs a slight perturbation to change because the aerodynamic forces help in moving the system away from its current state, making it easier to maneuver. Basically, there is a trade-off between the effort required to maintain an unstable motion and that of causing a stable motion to change, that is, between stability and maneuverability.

Whereas an assessment of the passive stability of live organisms is not feasible experimentally, an ingenious model system of an inanimate flyer was proposed recently as a proxy to flapping flight.[20,25,26] The experimental model consists of an upward-pointing pyramid-shaped object in a vertically oscillating airflow.[20,26] The inanimate flyer generates sufficient aerodynamic force to keep aloft and maintains balance passively during free flight. Liu *et al.*[20] use clever arguments and

a)Electronic mail: kanso@usc.edu

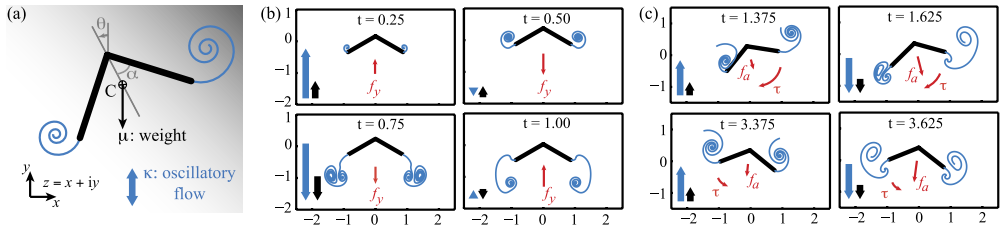

FIG. 1. (a) Λ-flyer hovering in oscillatory flow. Snapshots for (b) vertically upright flyer and (c) flyer initially tilted at an angle $\theta = 30°$. Black and blue (gray in print) arrows show the velocities of the flyer and the background flow, respectively. Aerodynamic force and torque are shown in red arrows (gray in print).

simplifying approximations founded on a deep understanding of aerodynamics to obtain "educated guesses" of the stabilizing mechanism without ever solving the coupled flow-structure interactions. In this work, we formulate a two-dimensional model of a Λ-shaped object in an oscillating uniform flow, see Fig. 1(a). This formulation enables us to quantitatively examine the aerodynamic forces required to keep the flyer aloft and the stabilizing aerodynamic moments. It also provides a framework for exploring optimal hovering conditions and studying the transition from unstable, yet more maneuverable, to stable hovering.

Our model Λ-flyer consists of two flat plates, of equal length l and total mass M (mass per length), joined at the apex at an angle 2α, see Fig. 1(a). The background fluid of density ρ_f oscillates vertically with velocity $U = A(\pi f)\sin(2\pi f t)$, where f is the oscillation frequency and A is the top-bottom oscillation amplitude. Four dimensionless parameters can be constructed: the mass $m = M/\rho_f l^2$ and weight $\mu = mg/lf^2$ of the flyer, and the amplitude $\beta = A/l$ and acceleration $\kappa = Af^2/g$ of the background flow. Note that the parameter κ can be interpreted as a measure of the *effort* needed to keep the flyer aloft. Let $z_c = x_c + \mathrm{i}y_c$ denote the position of the mass center C of the Λ-flyer in the complex z-plane ($\mathrm{i} = \sqrt{-1}$) and let θ denote its orientation from the upward vertical. The equations governing its free motion under the effects of gravitational and aerodynamic forces are

$$m\ddot{z}_c = f_x + \mathrm{i}(f_y - \mu), \quad I\ddot{\theta} = \tau, \tag{1}$$

where $I = m(1 - \frac{3}{4}\cos^2(\alpha))/3$ is the dimensionless moment of inertia; f_x, f_y, and τ are the aerodynamic forces and torque.[27]

We simulate the flow using a vortex sheet model in the inviscid fluid context.[27] The Λ-flyer is modeled as a bound vortex sheet that satisfies zero normal flow. A point vortex is released at each time step from the flyer's two outer edges, and the shed vorticity is modeled as a regularized free sheet.[27–32] No separation is allowed at the apex. Here, we follow the algorithm in Ref. 29 for imposing the Kutta condition that determines the amount of circulation shed from the outer two edges at each time step. The vortex sheet model depends on the regularization parameter for the free sheet, which we set to $\delta/l = 0.1$. By way of validation, we confirmed that our numerical scheme gives identical results for examples presented in Refs. 27 and 30 of driven and freely falling flat plates. Finally, to emulate the effect of viscosity, we allow the shed vortex sheet to decay gradually by dissipating each incremental point vortex after a finite time T_{diss} from the time it is shed in the fluid. Larger T_{diss} implies lower fluid viscosity. A closed-form expression that rigorously links T_{diss} to the kinematic fluid viscosity ν is not readily available; however, using approximate arguments based on the Lamb-Oseen solution, we choose T_{diss} such that νT_{diss} is small, where ν is the normalized viscosity of air. The effect of T_{diss} on the behavior of the flyer is discussed further in the end.

We first examine the behavior of a flyer undergoing periodic hovering motion. Fig. 1(b) depicts snapshots of the hovering motion and vortical wake for a flyer of angle $\alpha = 60°$ and mass $m = 8$ in an oscillating flow of amplitude $\beta = 1$, acceleration $\kappa = 6.5$, and dissipation parameter $T_{\mathrm{diss}} = 0.6$. The total simulation time is $t_{\mathrm{end}} = 40T$, where $T = 2\pi/f$ is the oscillation period of the background flow. The flyer is subject to zero initial velocity $\dot{x}_c(0) = \dot{y}_c(0) = 0$ and tilt conditions $\theta(0) = \dot{\theta}(0) = 0$. Clearly, during the upflow, vortices are generated at the two outer edges of the flyer. These vortices combine with the vortices generated during the downflow to form two vortex

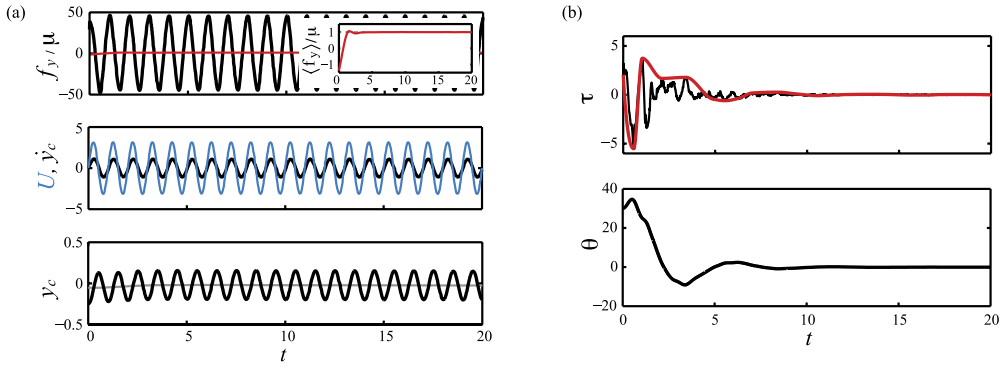

FIG. 2. (a) Periodic hovering of Fig. 1(b): normalized force, velocity, and position as functions of time. (b) Stable response of Fig. 1(c): The envelope (red) of the aerodynamic torque τ (black) fluctuates out of phase relative to the flyer's orientation θ.

dipoles that initially move vertically down. This downwash results in a lift force that balances the weight of the flyer, keeping it aloft as noted qualitatively in Ref. 20. Quantitatively, the aerodynamic torque τ and horizontal force f_x acting on the flyer are identically zero as expected from symmetry considerations while the vertical force f_y oscillates periodically from positive to negative at the same frequency as the background flow such that its T-averaged value $\langle f_y\rangle = \frac{1}{T}\left(\int_t^{t+T} f_y(\tilde{t})d\tilde{t}\right)$ when normalized by the flyer's weight μ is equal to $\langle f_y\rangle/\mu = 1$ (inset in Fig. 2(a) top). Vortex shedding is essential for the generation of these lift forces. The flyer responds by oscillating up and down at speeds smaller than those of the background oscillatory flow (Fig. 2(a) middle) such that it hovers around its initial vertical position. By hovering, we mean that the change in the T-averaged vertical position is equal to zero (gray line in Fig. 2(a) bottom).

This hovering motion is stable to initial perturbation, the tilt angle $\theta(0)$. Surprisingly, the flyer recovers the upright orientation and continues to hover stably for perturbations as large as $\theta(0) = 76°$. For $\theta(0) = 30°$, snapshots of the flyer and its wake during the recovery phase are depicted in Fig. 1(c). When the flyer is tilted to one side, the left-right symmetry of the shed vorticity is broken, which leads to stronger vorticity shed sideways from the edge with the larger angle of attack. The sideward vorticity creates a restorative aerodynamic torque as depicted quantitatively in Fig. 2(b). Both the torque envelope and the orientation of the flyer fluctuate out of phase relative to each other, indicating the restorative effect of the aerodynamic torque. The fluctuations decrease in amplitude and eventually approach zero as the flyer recovers its upright orientation.

We determine effective conditions for hovering as a function of two parameters: the flyer's shape described by the opening angle α and the *effort* or flow acceleration parameter κ. We set $m = 8$, $\beta = 1$ and we vary α from 10° to 90° and κ from 1 to 8. For a flyer of a given shape, there is an associated effort or flow acceleration that keeps the flyer aloft, starting in the upright position with zero initial velocity. Stronger or weaker efforts cause the flyer to ascend or descend. Each point (α, κ) represents one of three types of behavior: ascending ($\Delta y_c > 0$), hovering ($\Delta y_c = 0$), or descending ($\Delta y_c < 0$). The hovering condition $\Delta y_c = 0$ defines a *hovering curve* in the (α, κ)-plane as depicted in Fig. 3(a) for the case: $T_{\text{diss}} = 0.7$. There exists an optimal shape α_{op} for which the effort required to hover is minimum $\kappa = \kappa_{\text{min}}$. We then analyze the passive stability of all points on the hovering curve by imposing a small initial perturbation $\theta(0) = 1°$ and solving the fully nonlinear governing equations of motion in (1). In particular, we focus on the time evolution of the tilt angle θ: if it oscillates with decreasing or constant amplitude, we say the flyer is passively stable. If the amplitude of θ grows in time, the flyer is unstable. By mapping out these stability results to the hovering curve in Fig. 3(a), we see a transition from unstable to stable hovering as the opening angle of the flyer increases. Most importantly, the transition from unstable to stable hovering occurs at a critical shape α_{cr} that is post-optimal ($\alpha_{\text{cr}} > \alpha_{\text{op}}$), which leads to interesting insights into the interplay between maneuverability and stability in hovering flight.

Λ-flyers with aerodynamically optimal shapes α_{op} produce hovering motions that are passively unstable. One should therefore be careful when optimizing for aerodynamic effort without paying

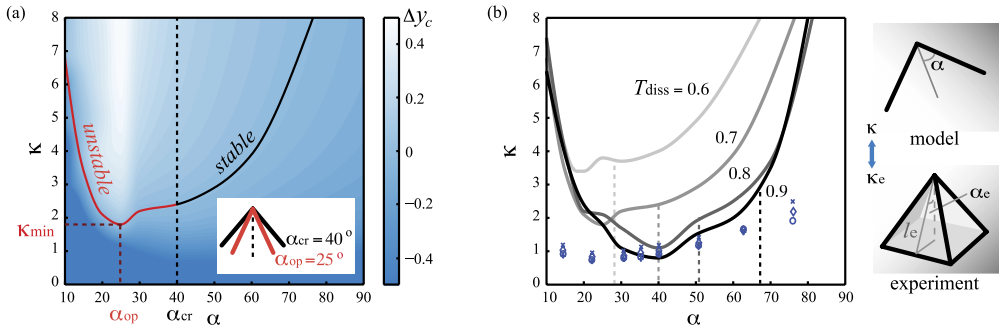

FIG. 3. (a) Parameter space (α, κ) for $T_{\text{diss}} = 0.7$. The *hovering curve* corresponds to vertically upright hovering ($\triangle y_c = 0$). Above ($\triangle y_c > 0$) and below ($\triangle y_c < 0$) this line, the flyer ascends and descends, respectively. Flyers of optimal shape α_{op} require minimum flow acceleration κ_{min} for hovering. A stability study shows a transition from unstable to stable hovering as α increases at $\alpha_{\text{cr}} > \alpha_{\text{op}}$. (b) Effect of T_{diss} and comparison with experimental data. Experimental hovering parameters α_e and κ_e are based on Weathers *et al.*[26] The $\circ$, $+$, $\times$, and $\diamond$ signs correspond to $f_e^{\circ} = 13$, $f_e^{+} = 15$, $f_e^{\times} = 20$, and $f_e^{\diamond} = 26$ Hz.

attention to motion stability. In so doing, one would obtain optimal flyers that, although more maneuverable, require active stabilization mechanisms. Active stabilization requires aerodynamic effort that may be even larger than the effort required for passive stability. This interpretation assumes that, when evaluating or designing flyers, one should opt for either stability or maneuverability. However, the results in Fig. 3(a) lend themselves to a far richer explanation. They suggest that a Λ-flyer that could actively change its shape, as in the case of live organisms, can smoothly switch from passively stable to unstable, yet more maneuverable, states by decreasing its opening angle. They also suggest that, although passive stability is not free (it comes at a higher effort κ), switching from stable to maneuverable states requires no extra effort, it rather requires a decrease in the aerodynamic effort κ because the transition α_{cr} occurs post-optimally for $\alpha_{\text{cr}} > \alpha_{\text{op}}$. Accordingly, we conjecture that, to fulfill the two requirements of passive stability and maneuverability, a good design practice both in nature and in man-made aerial vehicles is to position the stability limit at a post-optimal location in the parameter space.

To examine the effect of T_{diss}, we vary its value from 0.6 to 0.9 (see Fig. 3(b)). This choice of T_{diss} is consistent with Liu *et al.*[20] (Fig. 2), which suggests that the time scale of vorticity dissipation is close to one oscillation period. We compare our hovering conditions to the experimental results of Weathers *et al.*[26] (Fig. 6(a)). They considered a pyramid of mass $M_e = 0.224$ g, side length l_e, and apex angle α_e in flows oscillating at velocity $U_e = A_e(\pi f_e)\sin(2\pi f_e t)$, where the subscript e stands for experiment, and changed the shape of the pyramid such that $l_e \sin\alpha_e = 1.75$ cm. Based on these values, we construct the dimensionless parameters: $m_e = M_e/\rho_f l_e^3$, $\beta_e = A_e/l_e$, and $\kappa_e = A_e f_e^2/g$. The experimental values of α_e and κ_e are superimposed on Fig. 3(b) using different symbols $(\diamond, +, \times, \circ)$ corresponding to various oscillation frequencies f_e. Clearly, the data collapse after non-dimensionalization. As T_{diss} increases (viscosity decreases), the hovering curves for the Λ-flyer shift downwards and converge towards the experimental results. A smaller fluid viscosity, concomitant with a larger T_{diss}, delays vorticity dissipation, thus inducing a stronger interaction between the flyer and the surrounding fluid and requiring smaller flow acceleration to achieve hovering. Further, the optimal shape shifts to the right as T_{diss} increases. Interestingly, the optimal shape α_{op} (about 25°) for $T_{\text{diss}} = 0.7$ is close to the experimentally optimal shape. Note that the data reproduced from Weathers *et al.*[26] (Fig. 6(a)) correspond to a tethered pyramid and do not capture motion stability. In our model, the transition from unstable to stable hovering (dashed lines in Fig. 3(b)) shifts rightwards with increasing T_{diss}, consistent with the intuition that longer-lived vortical flows amplify instabilities. In all cases, the optimal shape is unstable, solidifying our conclusion that stable hovering is post-optimal.

The work of Y.H. and E.K. is partially supported by the NSF Grant No. CMMI 13-63404.

[1] C. P. Ellington, C. van den Berg, A. P. Willmott, and A. L. R. Thomas, "Leading-edge vortices in insect flight," Nature **384**, 626–630 (1996).
[2] M. H. Dickinson, F.-O. Lehmann, and S. P. Sane, "Wing rotation and the aerodynamic basis of insect flight," Science **284**, 1954–1960 (1999).
[3] G. Spedding, M. Rosén, and A. Hedenström, "A family of vortex wakes generated by a thrush nightingale in free flight in a wind tunnel over its entire natural range of flight speeds," J. Exp. Biol. **206**, 2313–2344 (2003).
[4] J. M. Birch and M. H. Dickinson, "The influence of wingwake interactions on the production of aerodynamic forces in flapping flight," J. Exp. Biol. **206**, 2257–2272 (2003).
[5] A. L. R. Thomas, G. K. Taylor, R. B. Srygley, R. L. Nudds, and R. J. Bomphrey, "Dragonfly flight: Free-flight and tethered flow visualizations reveal a diverse array of unsteady lift-generating mechanisms, controlled primarily via angle of attack," J. Exp. Biol. **207**, 4299–4323 (2004).
[6] D. R. Warrick, B. W. Tobalske, and D. R. Powers, "Aerodynamics of the hovering hummingbird," Nature **435**, 1094–1097 (2005).
[7] R. Ramamurti and W. C. Sandberg, "A three-dimensional computational study of the aerodynamic mechanisms of insect flight," J. Exp. Biol. **205**, 1507–1518 (2002).
[8] F. O. Minotti, "Unsteady two-dimensional theory of a flapping wing," Phys. Rev. E **66**, 051907 (2002).
[9] M. Sun and J. Tang, "Unsteady aerodynamic force generation by a model fruit fly wing in flapping motion," J. Exp. Biol. **205**, 55–70 (2002).
[10] M. Sun and S. L. Lan, "A computational study of the aerodynamic forces and power requirements of dragonfly (aeschna juncea) hovering," J. Exp. Biol. **207**, 1887–1901 (2004).
[11] Z. J. Wang, "Two dimensional mechanism for insect hovering," Phys. Rev. Lett. **85**, 2216–2219 (2000).
[12] Z. J. Wang, "Vortex shedding and frequency selection in flapping flight," J. Fluid Mech. **410**, 323–341 (2000).
[13] Z. J. Wang, J. M. Birch, and M. H. Dickinson, "Unsteady forces and flows in low Reynolds number hovering flight: Two-dimensional computations vs robotic wing experiments," J. Exp. Biol. **207**, 449–460 (2004).
[14] S. P. Sane, "The aerodynamics of insect flight," J. Exp. Biol. **206**, 4191–4208 (2003).
[15] Z. J. Wang, "Dissecting insect flight," Annu. Rev. Fluid Mech. **37**, 183–210 (2005).
[16] M. Sun, "Insect flight dynamics: Stability and control," Rev. Mod. Phys. **86**, 615–646 (2014).
[17] M. Sun and Y. Xiong, "Dynamic flight stability of a hovering bumblebee," J. Exp. Biol. **208**, 447–459 (2005).
[18] M. Sun, J. Wang, and Y. Xiong, "Dynamic flight stability of hovering insects," Acta Mech. Sin. **23**, 231–246 (2007).
[19] I. Faruque and J. S. Humbert, "Dipteran insect flight dynamics. Part 2: Lateral–directional motion about hover," J. Theor. Biol. **265**, 306–313 (2010).
[20] B. Liu, L. Ristroph, A. Weathers, S. Childress, and J. Zhang, "Intrinsic stability of a body hovering in an oscillating airflow," Phys. Rev. Lett. **108**, 068103 (2012).
[21] R. Dudley, "Mechanisms and implications of animal flight maneuverability," Integr. Comp. Biol. **42**, 135–140 (2002).
[22] L. Ristroph, A. J. Bergou, G. Ristroph, K. Coumes, G. J. Berman, J. Guckenheimer, Z. J. Wang, and I. Cohen, "Discovering the flight autostabilizer of fruit flies by inducing aerial stumbles," Proc. Natl. Acad. Sci. U. S. A. **107**, 4820–4824 (2010).
[23] J. A. Gillies, A. L. R. Thomas, and G. K. Taylor, "Soaring and manoeuvring flight of a steppe eagle aquila nipalensis," J. Avian Biol. **42**, 377–386 (2011).
[24] L. Ristroph, G. Ristroph, S. Morozova, A. J. Bergou, S. Chang, J. Guckenheimer, Z. J. Wang, and I. Cohen, "Active and passive stabilization of body pitch in insect flight," J. R. Soc., Interface **10**, 20130237 (2013).
[25] S. Childress, N. Vandenberghe, and J. Zhang, "Hovering of a passive body in an oscillating airflow," Phys. Fluids **18**, 117103 (2006).
[26] A. Weathers, B. Folie, B. Liu, S. Childress, and J. Zhang, "Hovering of a rigid pyramid in an oscillatory airflow," J. Fluid Mech. **650**, 415–425 (2010).
[27] M. A. Jones, "The separated flow of an inviscid fluid around a moving flat plate," J. Fluid Mech. **496**, 405–441 (2003).
[28] R. Krasny, "Desingularization of periodic vortex sheet roll-up," J. Comput. Phys. **65**, 292–313 (1986).
[29] M. Nitsche and R. Krasny, "A numerical study of vortex ring formation at the edge of a circular tube," J. Fluid Mech. **276**, 139–161 (1994).
[30] M. A. Jones and M. J. Shelley, "Falling cards," J. Fluid Mech. **540**, 393–425 (2005).
[31] S. Alben and M. J. Shelley, "Flapping states of a flag in an inviscid fluid: Bistability and the transition to chaos," Phys. Rev. Lett. **100**, 074301 (2008).
[32] S. Michelin, S. G. Llewellyn Smith, and B. J. Glover, "Vortex shedding model of a flapping flag," J. Fluid Mech. **617**, 1–10 (2008).